



Research Article

Evaluation of Mechanical Properties and Corrosion Resistance in Welded Stainless Steel 321H: Influence of Buttering Techniques

M. Beigi ¹, A. Khosravifard ^{*2}, A. Rabieezadeh ³, R. Sani ⁴*Department of Metallurgical and Materials Engineering, Engineering School, Shiraz Branch, Islamic Azad University, Shiraz, Iran*

ARTICLE INFO

Keywords:

Stainless Steel, Buttering, Mechanical Properties, Intergranular Corrosion.

Article history:

Received 17 November 2024

Received in revised form 03 January 2025

Accepted 28 April 2025

ABSTRACT

This study examines the mechanical properties and corrosion susceptibility of welded Stainless Steel 321H, focusing on the effects of buttering layers applied with NiCrMo filler metal compared to conventional welding without buttering. Tensile, bending, impact, hardness, and intergranular corrosion tests were conducted on both buttered and non-buttered samples. The results showed that non-buttered welds consistently exhibited superior strength and toughness, with ultimate tensile strengths ranging from 578 to 588 MPa and impact energy absorption values of 57.3 J to 67 J. In contrast, buttered samples demonstrated lower tensile strengths (560 to 578 MPa) and impact energy values (43 J to 51 J), underscoring the vulnerabilities introduced by the buttering process. Both sample types failed the intergranular corrosion tests, indicating that high heat input during welding contributes to sensitization. These findings highlight the need to optimize welding parameters to reduce sensitization and improve the mechanical and corrosion resistance of welded Stainless Steel 321H for demanding applications. While the buttering process facilitates the welding of dissimilar materials, its associated risks and limitations must be carefully considered.

1. Introduction

Stainless steels are renowned for their excellent mechanical properties and corrosion resistance, making them ideal for high-temperature applications in industries such as petrochemicals, aerospace, and power

generation [1, 2]. Among these materials, 321H stainless steel—a titanium-stabilized austenitic stainless steel—has gained prominence for its enhanced creep resistance and thermal stability, allowing it to perform effectively at temperatures up to 900 °C [3, 4]. However, high-temperature service conditions can pose significant challenges, particularly with respect to weld integrity and susceptibility to intergranular corrosion in the heat-affected zone (HAZ) adjacent to welds [5, 6]. Intergranular corrosion and Stress Relaxation Cracking (SRC) are well-documented phenomena that can degrade the mechanical properties and operational reliability of welded stainless-steel components [7, 8]. Sensitization occurs when stainless steels are exposed to temperatures between 425 °C and 850 °C, causing the precipitation of chromium carbides at grain boundaries. This depletes the surrounding areas of chromium, reducing corrosion

* Corresponding Author

Email: khosravifard@gmail.com

Address: Department of Metallurgical and Materials Engineering, Engineering School, Shiraz Branch, Islamic Azad University, Shiraz, Iran

1. Ph.D. Candidate, 2. Assistant Professor, 3. Associate Professor, 4. Assistant Professor

DOI: <http://10.22034/IJISSI.2025.2045999.1309>

Published by ISSI (Iron & Steel Society of Iran)

resistance [9, 10]. The thermal cycles of welding exacerbate this phenomenon, particularly in welded joints, where carbide precipitation increases susceptibility to intergranular attack [5, 11].

Buttering is a common industrial technique used for various purposes, such as welding dissimilar materials or improving the weldability of certain substrates. Therefore, it is crucial to evaluate its effects on welded joints. The primary objective of this study is to assess the mechanical properties and corrosion susceptibility of weld joints in Stainless Steel 321H, with and without buttering layers applied using NiCiMo filler metal. Previous research has shown that while buttering facilitates successful dissimilar metal welding, the associated microstructural changes require careful evaluation to mitigate sensitization in the base material [12-14]. These changes can significantly impact material toughness, ductility, and failure modes—critical considerations in the design and construction of pressure vessels and piping systems. This study seeks to expand the knowledge base on the effects of buttering on the mechanical properties of 321H stainless steel welds. Through comprehensive mechanical testing and detailed microstructural analysis, it aims to clarify the relationship between buttering, weld quality, and sensitization risks, ultimately providing insights to guide industry practices and improve fabrication standards.

2. Experimental section

2.1. Materials

The investigation utilized ASTM A312-TP321H stainless steel, a material widely used in high-temperature applications for its excellent mechanical properties, oxidation resistance, and ability to maintain structural integrity under stress. The selection of this grade highlights its importance in industries such as petrochemicals

and power generation, where components must withstand extreme operational conditions. NiCiMo filler metal was used for buttering, while 16-8-2 filler metal was employed for the main weld, with their chemical compositions detailed in Table 1.

2.2. Welding Procedure

The welding process was carefully executed to ensure reproducibility and reliability in assessing the buttering effect on weld mechanical properties. Before welding, the base materials were meticulously cleaned to remove oxide layers and contaminants that could compromise weld quality. The buttering layer was applied using NiCiMo filler metal, deposited on the prepared bevel edges of the stainless-steel pipes.

The buttering process involved multiple controlled passes with low heat input to ensure thorough fusion without compromising the metallurgical properties of the base material. This was performed using the Gas Tungsten Arc Welding (GTAW) process, renowned for its precise control over heat input and welding speed. After applying the buttering layer, the primary weld was completed using the 16-8-2 filler metal, also employing the GTAW method. Welding parameters were selected in accordance with conventional industrial practices, as detailed in Table 2.

2.3. Microstructural Analysis

Optical Microscopy (OM): The samples were ground using SiC grit paper to a 5000-grit finish and polished with a 1- μ m alumina suspension. They were then etched with a 10% oxalic acid solution for 30 seconds. An Olympus PMG3 optical microscope was used to analyze the grain structure, phase distribution, and potential signs of sensitization.

Table 1. Chemical composition of the welded material and fillers used.

Material	C (wt.%)	Si (wt.%)	Mn (wt.%)	S (wt.%)	P (wt.%)	Cr (wt.%)	Ni (wt.%)	Mo (wt.%)	Ti (wt.%)
AISI 321H	0.04-0.10	1.00	2.00	0.030	0.045	17.0-19.0	9.0-12.0	-	5 x %C
NiCiMo Filler metal	0.05	0.75	2.00	0.01	0.02	12.0	6.0	2.0	-
16-8-2 Filler metal	0.06	0.40	1.40	0.01	0.01	15.5	8.5	1.3	-

Table 2. WPS Used for Welding.

Weld Pass	Process	Diameter, mm	Type and Polarity	Current Range, A	Voltage Range, V	Travel Speed Range, mm/min
Buttering	GTAW	2.4	DC-EN	90-110	10-12	60-100
1	GTAW	2.4	DC-EN	90-110	10-12	60-100
2	SMAW	2.5	DC-EP	60-90	22-24	140-160
3	SMAW	3.2	DC-EP	80-120	23-25	180-200
2-n	SMAW	4.0	DC-EP	100-150	24-26	200-240

Additional Parameters:

- Shielding and Backing Gas: Argon (99.99%) with a flow rate of 10-15 L/min.
- Interpass Temperature: Maximum 150 °C.
- Type of Joint: Butt weld with a beveling angle of $70 \pm 5^\circ$.
- Note: The parameters for the buttering row apply only to the buttered material.

Scanning Electron Microscopy (SEM): High-resolution images were captured using a Philips XL30 SEM to analyze the microstructure at a granular level. The examination focused on the weld interface and buttering layer, identifying voids, inclusions, or detrimental microstructural features such as chromium carbide precipitation along grain boundaries. Energy Dispersive X-ray Spectroscopy (EDS) mapping and point analyses were conducted during SEM imaging to quantify elemental distributions within the weld joint components, with particular emphasis on the buttering layer and heat-affected zone (HAZ). This analysis provided critical insights into elemental changes and potential segregation phenomena resulting from the welding process.

2.4. Mechanical Testing

Once welding was completed, the samples underwent rigorous mechanical testing to evaluate the effects of buttering on weld properties.

The tensile properties of the welded specimens were measured according to ASTM E8/E8M standards, which outline guidelines for tensile testing of metallic materials. The tests were conducted using a Hounsfield H50KS universal testing machine, known for its precision and reliability in materials testing. The machine operated at a constant crosshead speed of 1 mm/min to ensure controlled strain rates during testing.

Bending tests were performed to evaluate the toughness of the welds and their resistance to cracking under applied loads, using a SATEC bending testing machine. The details of the testing parameters are provided in

Table 3. A three-point bending configuration was employed, widely recognized for its effectiveness in evaluating flexural properties. To ensure accurate results, the deflection rate was carefully controlled to minimize the influence of dynamic loading effects.

The Charpy V-notch test was conducted following ASTM E23 guidelines, using an Instron 3400 Series machine. This test aimed to evaluate the impact resistance of the welded joints under varying temperature conditions, specifically at room temperature and sub-zero temperatures. Samples were prepared with dimensions of 10 mm x 10 mm x 55 mm, adhering to the specifications for Charpy V-notch testing.

Vickers hardness tests were performed on various locations within the welded sections, specifically targeting the base metal, the heat-affected zone (HAZ), and the weld metal itself. These tests were conducted using a Buehler MicroMet 5101 hardness testing machine, known for its precision and accuracy in measuring material hardness. To obtain a comprehensive understanding of the hardness profile, measurements were taken at multiple points across the cross-section of each sample.

2.5. Corrosion Properties

In order to further evaluate the risk of sensitization, intergranular corrosion testing (IGC) was utilized in accordance with ASTM A262 Practice E standards. The procedure involved immersing the samples in a boiling solution of copper sulfate mixed with sulfuric acid for a specified duration (15 hours). After exposure, the specimens were subjected to a bending test to identify any

intergranular cracks or signs of corrosion along the welded areas. The results were visually assessed, and microstructural examinations were conducted on the bent areas to confirm any signs of susceptibility.

3. Results and Discussion

3.1. Microstructural Studies

3.1.1. Metallography of the Buttered Material

Fig. 1. provides a comprehensive overview of the microstructural characteristics of the buttered sample, highlighting the distinct regions from the base metal to the weld area, observed at various magnifications.

Fig. 1(a). shows the microstructure of the buttered sample includes the base metal, heat-affected zone (HAZ), buttering layer, and weld area at a magnification of X100. This view illustrates the continuity and transitions among these critical zones, emphasizing how thermal and compositional variations affect the overall integrity of the joint.

At a higher magnification of X500 (Fig. 1(b).), the fusion line and buttering area reveal the presence of carbonitride particles. These particles, primarily composed of titanium and niobium, play a vital role in enhancing mechanical properties by improving hardness and strength, particularly at the interfaces where different materials meet. This has been noted in previous studies; for instance, Liu et al. [14] emphasize the role of these particles in enhancing strength and toughness in dissimilar metal welds, underscoring their importance during the welding process. Their findings support the microstructural observations made in Fig. 1. specifically in the context of the enhanced properties attributed to secondary microstructural phases.

According to Fig. 1(c). the microstructure exhibits a well-defined austenitic structure characterized by twinning zones and delta ferrite strands, consistent with findings from similar studies [2]. The presence of these features, observed at X100, indicates the influence of alloying elements and cooling rates during processing, which contribute to phase stability and the mechanical performance of the base metal. The prominence of twinning zones may indicate specific cooling rates and alloy composition effects, as discussed by Gajjar et al. [1], who highlight the impact of thermal cycles on sensitization and austenite microstructures.

In the buttering zone, observed at a magnification of X500 (Fig. 1(d).), the structure demonstrates a solid solution austenitic form with a significant presence of titanium and niobium carbonitrides. This solid solution strengthens the buttering layer, ensuring it adequately prepares the base metal for the subsequent welding process. The absence of noticeable defects in this area is crucial, as it contributes to the overall effectiveness of the weld joint.

Micrographs illustrating these observations provide

valuable insights into the microstructural integrity of the buttered welds. These observations identify potential areas that could impact mechanical properties, including the presence of carbonitrides, which may influence performance under stress.

The metallographic examination of the buttered materials indicates that while buttering improves compatibility in dissimilar metal joints, the resultant microstructural complexities—such as twinning and delta ferrite formations—must be considered for their potential impact on weld integrity. The presence of titanium and niobium carbonitride particles in the butter zone further emphasizes the need for careful evaluation of material behavior under service conditions, as supported by previous studies [5, 6].

3.1.2. Metallography of the Non-Buttered Material

Fig. 2. provides a comprehensive metallographic examination of the welded material without a buttering layer, highlighting important microstructural characteristics across different regions of the sample.

Fig. 2(a). reveals an austenitic structure characterized by twinning zones and delta ferrite islands. These features are critical, as they can substantially influence the mechanical properties and corrosion resistance of the welded joint. The presence of fine titanium carbonitride-rich deposits further signifies the complexity of the microstructure, consistent with findings by other researchers [1], who highlighted the role of such deposits in enhancing strength and toughness in austenitic stainless steels.

The base metal adjacent to the heat-affected zone (HAZ) retains its characteristic austenitic structure, with identifiable twinning zones and delta ferrite islands (Fig. 2(b)). These observations align with studies by other researchers [2], who emphasize the significance of microstructural stability in mitigating the risk of sensitization and maintaining mechanical integrity after welding. The presence of delta ferrite suggests a complex microstructure that may be prone to variations in mechanical performance, particularly under thermal stress conditions.

A focused examination of the HAZ at high magnification reveals critical changes in the microstructure arising from the thermal effects of welding (Fig. 2(c)). The observed twinning zones and delta ferrite islands underscore the complexities of this region. This aligns with research by Chabaud-Reyter et al. [7], who discussed stress relief cracking mechanisms in austenitic stainless steels. Such insights are vital for predicting the long-term behavior of weld joints exposed to operational stresses.

The weld area exhibits a clear austenitic structure integrated with distinct delta ferrite islands (Fig. 2(d)). The variations in solidity indicated by these microstructural features raise potential concerns about the quality and reliability of fusion in the weld zone.

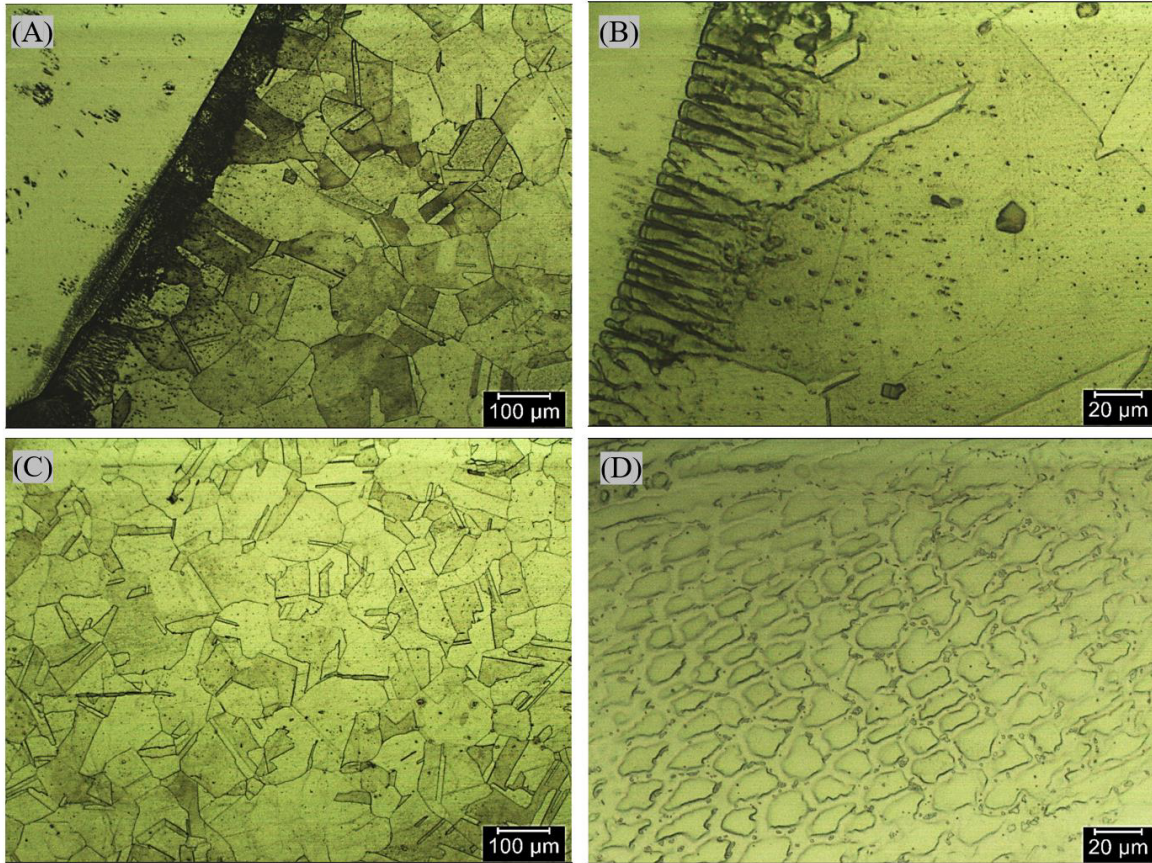


Fig. 1. (a) Overall Microstructure of buttered sample including the base, HAZ, Buttering, and weld area, X100. (b) Presence of Carbonitrides in the fusion line and Buttering area, X500. (c) The austenitic structure along with twinning zones and delta ferrite strands in the base metal, X100. (d) Buttering area in a higher magnification X500.

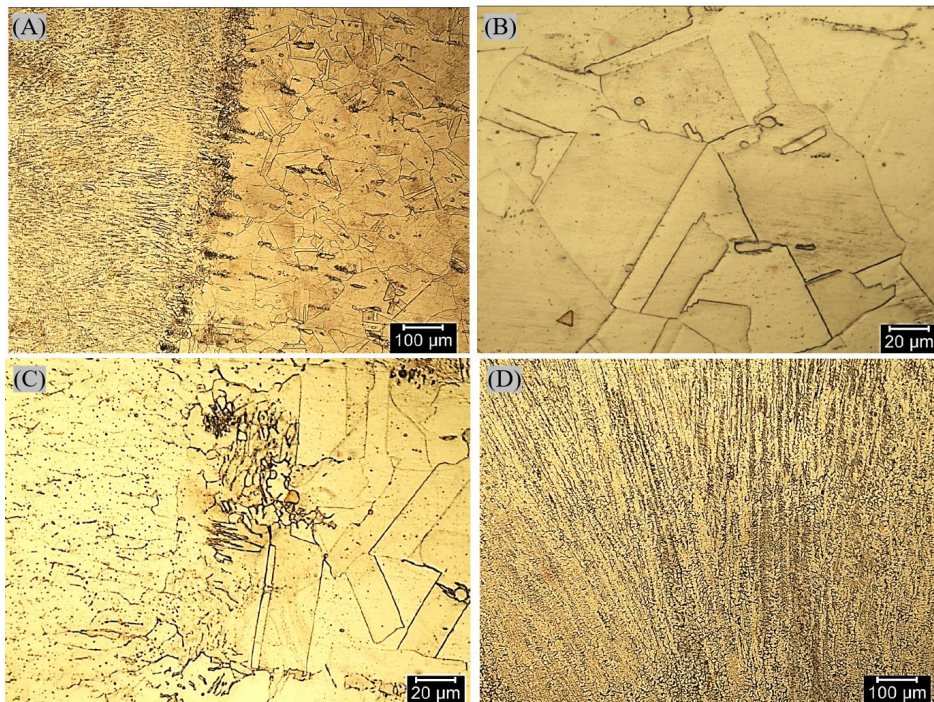


Fig. 2. (a) Overall Microstructure of welded material without Buttering. (b) Microstructure of base metal the areas new to HAZ. (c) High magnification of HAZ area. (d) The Weld area of sample without buttering.

3.2. SEM and EDS Analysis of Buttered Samples

The Scanning Electron Microscopy (SEM) images and Energy Dispersive X-ray Spectroscopy (EDS) results for the buttered samples corroborated the observations made during the metallographic examination. The SEM provided high-resolution images that revealed detailed microstructural features, as shown in Fig. (3-7). with the following detailed explanation.

Fig. 3. is an SEM image with a macro view capturing an area at a 2mm magnification scale. This image effectively displays the different zones within the sample: the buttering layer, the weld metal, and the base material. The SEM image provides a comprehensive view of the sample's surface, clearly distinguishing between the buttering layer and the weld metal. This macro-scale image is valuable for understanding the spatial relationship between these regions. The buttering layer, applied to prepare the surface for welding, and the subsequent weld metal are clearly visible and distinct in the image. This delineation is crucial for quality control and assessing the uniformity of the applied layers. Despite the clarity in observing the layers, the image also reveals some imperfections, including possible porosity, cracks, inclusions, or other discontinuities in the weld and buttering areas. Such defects can negatively impact the mechanical properties and overall integrity of the welded joint, making their identification essential for subsequent analysis and corrective actions.

Fig. 4. presents a detailed examination of the microstructure of the base metal, along with Energy Dispersive Spectroscopy (EDS) analyses performed at two distinct points within the sample. This figure highlights compositional variations and provides valuable insights into

the material's microstructural characteristics. The microstructure visible in Fig. 4. reveals the grain structure and potential phase distributions within the base metal.

EDS analysis of matrix: The EDS results for matrix indicate a predominance of iron (Fe) at 66.11%, which aligns with the expected composition of the base metal. This high iron content, coupled with notable chromium (Cr) at 18.75%, suggests the presence of a chromium-rich phase, which likely contributes to corrosion resistance. Nickel (Ni) is also present at 9.30%, indicating its role in alloying the base metal to enhance toughness and resilience. The smaller amounts of aluminium (Al), silicon (Si), and manganese (Mn) further influence the material's strength and ductility. The presence of molybdenum (Mo) at 1.92% suggests a potential contribution to the material's strength and resistance to pitting corrosion, which is common in stainless steels.

EDS analysis of selected islands: In contrast, the EDS results of selected islands show a very high nitrogen (N) content at 71.76%, which is unusual for typical base metals but may indicate a nitriding process or the presence of a nitrogen-rich phase. Titanium (Ti) is also significantly present at 27.71%, suggesting the formation of titanium nitrides or other titanium-based compounds. These contribute to the hardness and reinforcement of the microstructure. The minimal amounts of chromium and iron detected in this region (0.28% Cr and 0.24% Fe) imply that this area is enriched with titanium and nitrogen, rather than being representative of the bulk metal composition.

Fig. 5. presents the microstructure and EDS analyses of selected points within the heat-affected zone (HAZ) and the weld area. This figure is essential for understanding compositional changes and microstructural integrity during welding, particularly in regions adjacent to the weld.

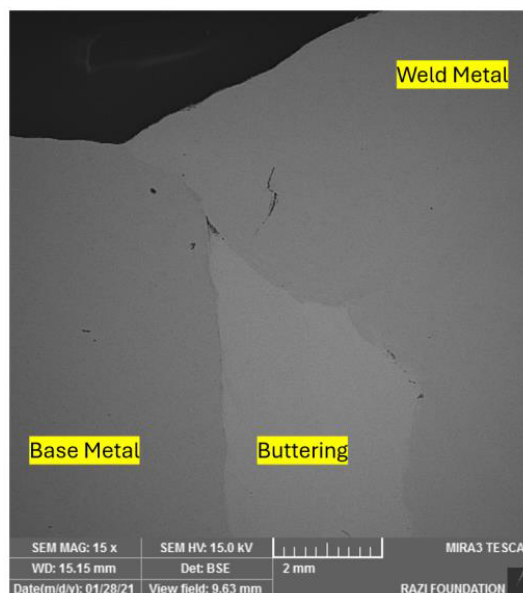


Fig. 3. SEM image showing the overall view of the buttered sample.

The HAZ microstructure reveals a network of chromium-rich phases within an austenitic matrix, which can alter grain size, phase distribution, and potentially form new phases. Examining this area provides insight into how weld parameters influence the structural properties of the base metal. EDS analysis shows Fe as the predominant element at 66.30%, consistent with the base material, indicating typical HAZ composition. On the other hand, Cr is present at 18.68%, suggesting that chromium-rich phases crucial for corrosion resistance are retained in the HAZ. Also, Ni Constitutes 9.11%, enhancing toughness and strength in these regions. Furthermore, lower concentrations of aluminium (Al), silicon (Si), titanium (Ti), and manganese (Mn) are observed, indicating their roles as stabilizing or strengthening elements. Niobium (Nb) and molybdenum (Mo) appear in trace amounts, contributing to improved strength and corrosion resistance, beneficial in welded structures.

EDS analysis at a selected point in the weld zone shows Fe Predominant at 54.06%, though lower than in the HAZ, likely due to dilution effects in the weld pool. Also, Ni is present at a higher amount of 14.81%,

reflecting contributions from the filler metal to weld properties. Cr Maintains a significant presence at 18.97%, preserving corrosion-resistant properties. Furthermore, minimal amounts of aluminium (0.49%), silicon (0.99%), and titanium (0.28%) suggest reduced influence on the weld metal compared to the base metal. Mo increased to 7.90% in the weld area, likely enhancing localized corrosion resistance and mechanical properties.

Fig. 6. illustrates the microstructure of the buttering area in the weld joint, accompanied by EDS analyses performed on a selected point within this region. The EDS analysis shows Ni as most abundant element, comprising 29.18% of the composition. This high nickel content is critical for enhancing ductility and toughness, particularly in high-temperature or corrosive environments. Mo Present at 25.42%, plays a significant role in strengthening and improving the corrosion resistance of the buttering layer. Nb accounts for 21.95%, contributing to grain refinement and overall mechanical strength, which helps stabilize the microstructure. Cr found at 13.27%, is essential for corrosion resistance. The relatively lower chromium content may indicate variations in the

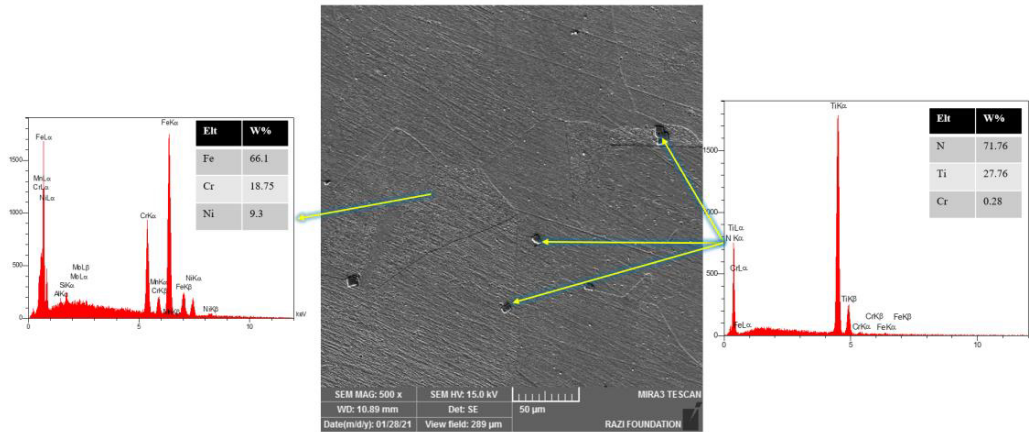


Fig. 4. The Microstructure and EDS analyses of the points shown in the Base metal.

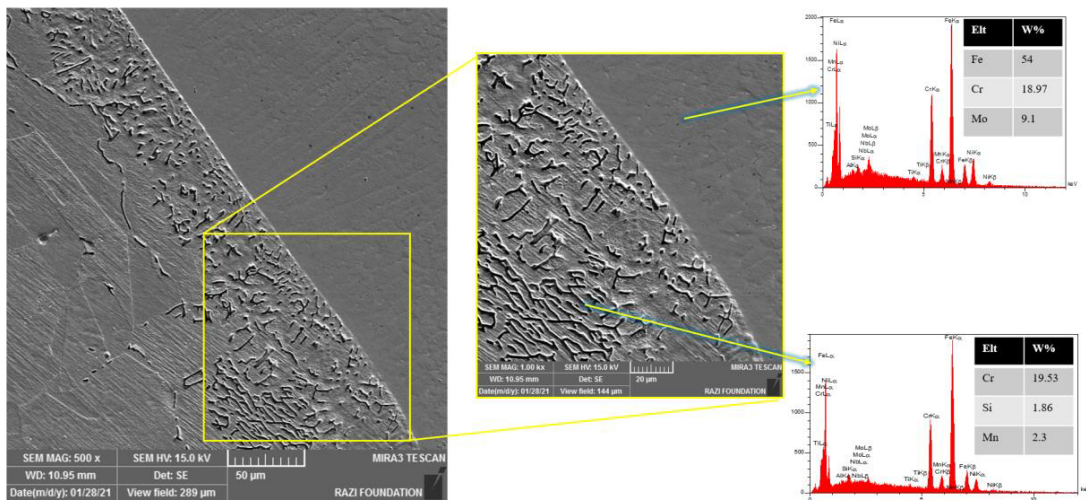


Fig. 5. The Microstructure and EDS analyses of the points shown in the HAZ area.

buttering material, potentially influencing performance compared to the base and weld metals. Si and Fe are present at 1.28% and 8.91%, respectively. While silicon enhances fluidity during welding, the lower iron content suggests that the buttering material is primarily based on nickel alloys rather than ferrous components.

The EDS results in Fig. 7. highlight a very high oxygen content (70.22%) in one of the selected points, accompanied by significant amounts of titanium (Ti), manganese (Mn), and chromium (Cr), as well as smaller amounts of aluminum (Al), silicon (Si), and iron (Fe). This composition suggests the formation of various oxide phases and related compounds as will be discussed here. But it should be emphasized that presence of all these phases needs to be confirmed by further examinations such as XRD. The significant presence of titanium and oxygen strongly indicates the formation of titanium dioxide (TiO₂), a stable and common phase in oxidizing environments. On the other hand, the presence of aluminum and silicon, though in smaller quantities, suggests the potential formation of alumina (Al₂O₃) and silica (SiO₂). Also, Chromium readily forms oxides, especially in oxygen-rich conditions, contributing to corrosion resistance. The presence of Mn, Cr, Al, and Fe suggests

the potential formation of spinel-type structures, such as MnCr₂O₄ or Mn₃O₄. These are commonly associated with high-temperature oxidation environments. Furthermore, the presence of Al and Si raises the possibility of forming silicates or aluminosilicates. However, these would likely constitute minor phases due to their relatively low concentrations.

In contrast, another selected point in Fig. 7. reveals high amounts of niobium (Nb) and molybdenum (Mo), along with significant portions of chromium (Cr), iron (Fe), and smaller amounts of nickel (Ni) and manganese (Mn). Based on this composition, the following phases may have formed: The high niobium and chromium content suggest the formation of NbC or Cr-rich carbides (e.g., Cr₂₃C₆). These carbides are typical in stainless steels and weld regions, contributing to wear resistance. Also, Sigma (σ), an intermetallic phase, rich in chromium and molybdenum, can form in stainless steels exposed to elevated temperatures. While it enhances strength, its presence may also lead to embrittlement. The high niobium and the presence of nickel point to the possibility of Laves phases, such as Ni-Nb intermetallics. These are often observed in Ni-based superalloys or weld deposits containing Nb.

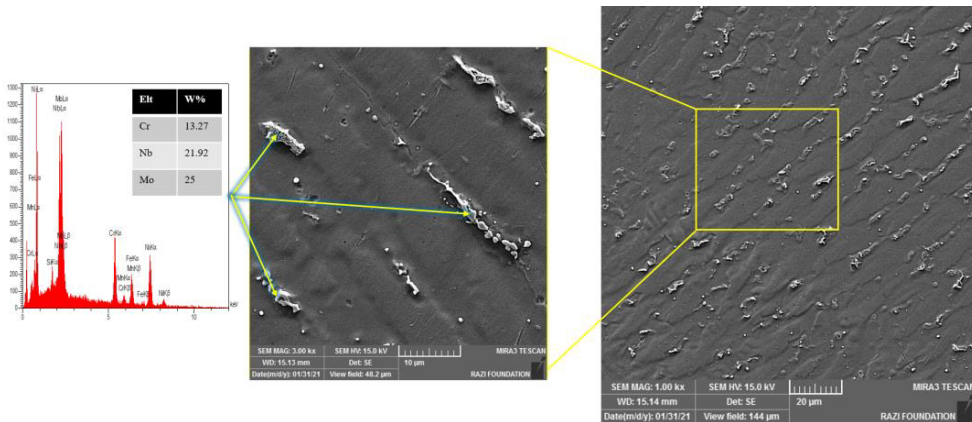


Fig. 6. The Microstructure and EDS analyses of the points shown in the Buttering area.

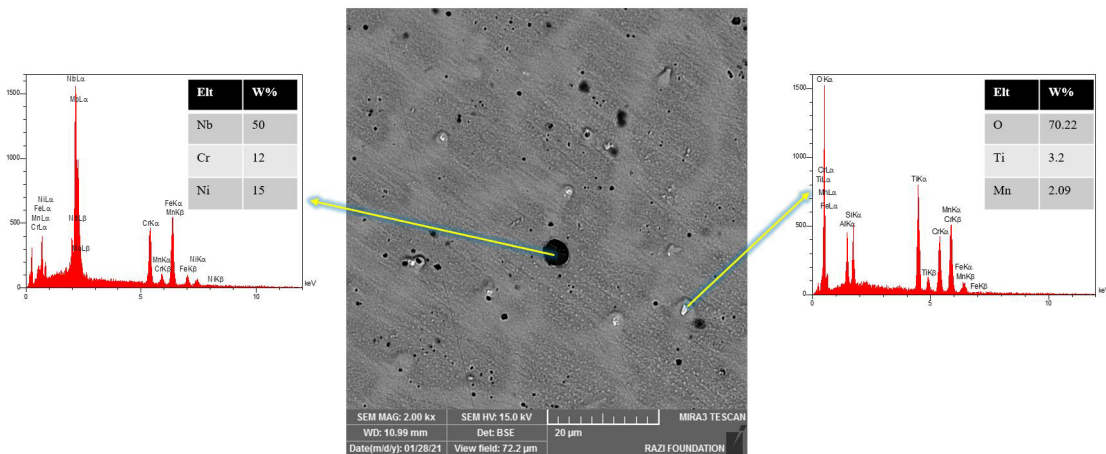


Fig. 7. The Microstructure and EDS analyses of the points shown in the Weld area.

3.3. Mechanical Test Results

3.3.1. Tensile Test

The tensile test results of the welded samples reveal notable differences between buttered and non-buttered conditions, as is obvious in engineering stress-strain curves shown in figs. 8 and 9., respectively.

- Buttered Samples: The ultimate tensile strength (R_m) of the buttered samples ranged from approximately 560 to 578 MPa, with a 0.2% proof strength (Y_S) between 312 and 372 MPa. While buttering offers compatibility benefits, it also introduces challenges in maintaining mechanical integrity.

- Non-Buttered Samples: The results for the non-buttered samples show a slightly higher ultimate tensile strength (R_m), ranging from 578 to 588 MPa, and higher proof strength (Y_S) values between 329 and 386 MPa. These findings indicate that non-buttered welds generally exhibit superior mechanical properties, which are critical in structural applications.

The comparison of tensile strengths highlights that non-buttered samples consistently demonstrate better performance in strength metrics. Several factors contribute to this observation: 1) Microstructural Integrity:

Metallographic analysis indicates that non-buttered welds maintain a more consistent austenitic structure without disruptions caused by the buttering layer. Studies suggest that non-buttered welds often exhibit a more homogeneous microstructure, which enhances mechanical performance [12]. 2) Presence of Carbonitride Particles: The buttered samples contain significant quantities of titanium and niobium carbonitride particles. While these particles may enhance certain localized aspects of the microstructure, they can also act as nucleation sites for cracks, thereby reducing overall tensile strength [5, 6]. 3) Welding Parameters: Variations in welding parameters associated with both processes play a crucial role in determining mechanical properties. Excessive heat input during welding, particularly during the buttering phase, can lead to detrimental microstructural changes such as grain coarsening, which result in reduced strength [8, 9]. 4) Industry Practices: Insights from these findings align with literature emphasizing the importance of carefully evaluating buttering applications in critical welds. Buttering should not only be assessed for its ability to enhance compatibility but also for its potential effects on the mechanical properties of the weld joint [10].

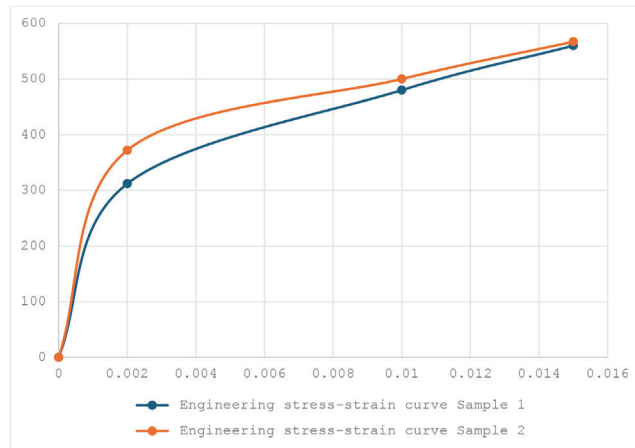


Fig. 8. Engineering stress-strain curves, Vertical axis: Engineering Stress (σ), Horizontal axis: Engineering Strain (ϵ) of the Welded Samples with Buttering

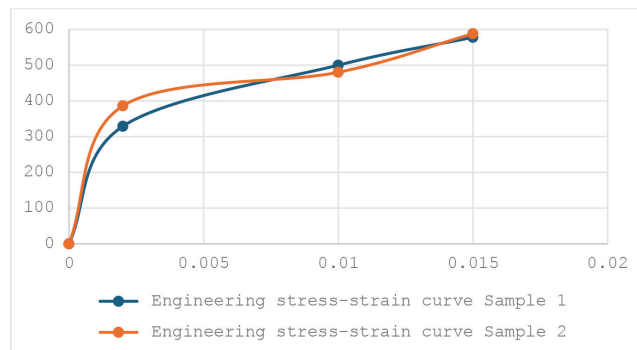


Fig. 9. Engineering stress-strain curves, Vertical axis: Engineering Stress (σ), Horizontal axis: Engineering Strain (ϵ) of the Welded Samples without Buttering.

3.3.2. Bending Test Results

The bending test results, presented in tables 3 and 4 for both sample types, provide insights into the ductility and toughness of the welds.

- **Buttered Samples:** The bending tests on the buttered samples revealed significant susceptibility to cracking, as all tested samples failed. This indicates weaknesses in the welded regions due to the presence of the buttering layer. The failure modes were primarily localized in the bending area, highlighting imperfections introduced during the welding process.

- **Non-Buttered Samples:** In contrast, the non-buttered samples successfully passed the bending test, showing no observable defects or signs of weakness. This performance demonstrates that the non-buttered welds preserved greater structural integrity and ductility under loading conditions.

The bending test results reveal substantial differences in the performance of buttered versus non-buttered welded samples. Several factors contribute to these observations: 1) **Microstructural Integrity:** The buttering process may introduce additional complexities in the microstructure, such as the formation of hard titanium nitride or carbonitride particles, which act as stress concentrators.

These features can compromise mechanical behavior during bending, resulting in premature failure. In contrast, the non-buttered samples retained a more uniform austenitic structure, which is less prone to localized failures [8, 9]. 2) **Effect of Welding Parameters:** The welding parameters used during the buttering process significantly influence the mechanical response of the weld. Excessive heat input or improper interpass temperatures can promote the formation of brittle phases or residual stresses, increasing the weld's susceptibility to cracking under bending loads [10, 11]. Non-buttered samples, which avoid the additional buttering step, are likely to experience reduced thermal gradients and stress concentration effects. 3) **Industry Practices:** Previous studies have indicated that while buttering enhances compatibility for dissimilar materials, it can reduce the toughness of welded joints when not optimized [12]. It is therefore crucial to carefully assess the implications of buttering in critical welding applications.

3.3.3. Hardness

The hardness test results, presented in Fig. 10. for both buttered and non-buttered samples, provide critical insights into the mechanical properties under these

Table 3. Bending Test Results for the Welded Sample with Buttering.

Sample ID	Test Result	Remarks	Angle of Bend (Degrees)	Size (Thickness x Width) (mm x mm)	Sample Location
Sample 1	Reject	A crack of length 3.20 mm observed at the weld.	180	54 x 10	Side I
Sample 2	Reject	Cracks of lengths 3.56 mm and 2.96 mm observed at the weld.	180	54 x 10	Side II
Sample 3	Reject	Cracks of lengths 3.43 mm and 2.93 mm observed at the weld.	180	54 x 10	Side III
Sample 4	Reject	Cracks of lengths 4.71 mm and 3.40 mm observed at the weld.	180	54 x 10	Side IV

Table 4. Bending Test Results for the Welded Sample without Buttering.

Sample ID	Test Result	Remarks	Angle of Bend (Degrees)	Size (Thickness x Width) (mm x mm)	Sample Location
Sample 1	Accept	No defects observed	180	54 x 10	Side I
Sample 2	Accept	No defects observed	180	54 x 10	Side II
Sample 3	Accept	No defects observed	180	54 x 10	Side III
Sample 4	Accept	No defects observed	180	54 x 10	Side IV

conditions.

- **Buttered Samples:** The hardness measurements for the buttered samples showed a range of values, with average levels approximately between 176 and 197 HV across various zones, including the base material and weld metal. The presence of titanium and niobium carbonitride particles was noted, which may influence hardness distribution and overall material behavior.

- **Non-Buttered Samples:** In contrast, the non-buttered samples exhibited slightly higher hardness values, with ranges typically from 170 to 213 HV. This indicates that the non-buttered welds maintained superior overall mechanical properties, likely due to a more uniform microstructure and a reduced presence of stress concentrations.

The comparison of hardness values between buttered and non-buttered samples highlights several important aspects: 1) **Microstructural Effects:** The austenitic structure of the non-buttered samples, characterized by a consistent grain structure, likely contributed to their better hardness results. In contrast, the buttered samples, influenced by the addition of the buttering layer, exhibited variations in hardness, suggesting localized softening or hardening effects arising from distinct microstructural characteristics [13, 14]. 2) **Contributions from Alloying Elements:** The buttered samples contained titanium and niobium carbonitride precipitates, which, while beneficial for specific properties, may also induce heterogeneity in the hardness profile. This can lead to localized variations and potential weaknesses. Studies on stainless steel under service conditions emphasize the impact of these precipitates on hardness distribution [12]. 3) **Welding Process Influence:** Differences in heat input and cooling rates during welding can significantly affect the hardness of the weld zone. Non-buttered samples might have undergone more uniform cooling cycles, resulting

in more favorable hardness values. Conversely, buttered samples could have experienced uneven thermal conditions, influencing crystal structure transformations and leading to inconsistent hardness [9, 15, 16].

The hardness test results highlight notable differences between buttered and non-buttered welded samples, with non-buttered samples generally exhibiting superior hardness values. The presence of distinct microstructures, alloying elements, and variations in welding processes play critical roles in shaping these mechanical properties. To optimize welding procedures and material selection for industrial applications, it is crucial to consider the implications of hardness variations introduced by buttering and ensure a comprehensive evaluation of the microstructural integrity of welded joints [17].

3.3.4. Impact test results

The results of the Charpy impact tests, as shown in Fig. 11. reveal significant differences in toughness between the buttered and non-buttered welded samples, which are critical for assessing their performance under dynamic loading conditions.

- **Buttered Samples:** The Charpy impact tests on the buttered samples recorded energy absorption values ranging from 43 J to 51 J at -196 °C, indicating moderate toughness. However, these samples displayed a tendency for crack formation during loading, potentially compromising their structural integrity in service.

- **Non-Buttered Samples:** By comparison, the non-buttered samples exhibited superior energy absorption, with values ranging from 57.3 J to 67 J at the same temperature. This improved performance suggests a more resilient material under impact conditions, likely attributed to a more uniform microstructure and a reduced presence of flaw concentrations.

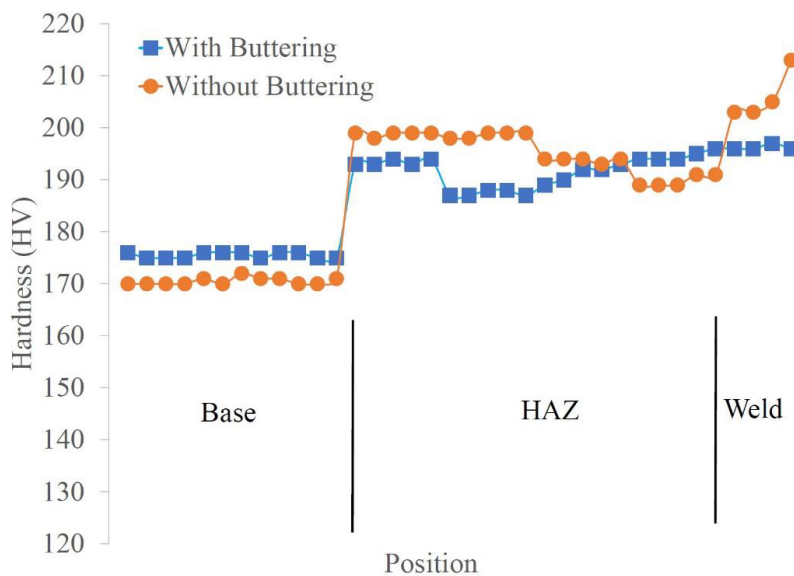


Fig. 10. Vickers hardness values obtained at various locations of the welded samples with and without buttering.

The discrepancies in impact test results emphasize critical material behavior under stress:

- **Microstructural Implications:** The presence of carbonitride particles in the buttered samples may have localized the toughness, causing a decrease in energy absorption. Studies have shown that such microstructural features often lead to reduced toughness, correlating directly with mechanical performance indicators [12, 18-20].

- **Welding Parameters and Heat Input:** Variations in welding parameters during the buttering process can create microstructural weaknesses that manifest as decreased impact toughness. Excessive heat input in buttered samples may lead to embrittlement, which is supported by the tighter ranges observed in their impact results. Conversely, non-buttered samples may benefit from a more controlled thermal cycle, optimizing their toughness without compromising integrity [11, 21].

- **Consistency Across Tests:** As indicated in the hardness results, where non-buttered samples exhibited slightly higher hardness values—often correlated with better overall mechanical performance—these trends are mirrored in the impact test outcomes. The non-buttered samples not only maintained higher hardness levels but also demonstrated superior impact resistance, reinforcing the notion that strength and toughness are interrelated [22].

3.4. Intergranular Corrosion Tests

The results of the Intergranular Corrosion tests (IGC) indicate notable implications regarding the susceptibility of the welded samples to corrosion, despite the presence of a buttering layer intended to enhance compatibility. Both the buttered and non-buttered samples failed the IGC test, demonstrating considerable vulnerability to intergranular corrosion, as shown in Figs. 12 and 13. In

both cases, the microstructural analysis (Figs. 12(a) and 13(a)) corresponds to the "ditch" microstructure pattern described in the ASTM A262 standard. The bending test results (Figs. 12(b) and 13(b)), clearly show the presence of cracks and surface imperfections, leaving no ambiguity.

As highlighted in another article by the same authors [21], the selection of welding parameters plays a crucial role in controlling heat input during the welding process. Excessive heat input can cause sensitization in austenitic stainless steels, leading to the formation of chromium carbides along grain boundaries. This sensitization significantly reduces the material's corrosion resistance, particularly in the heat-affected zone (HAZ), as demonstrated in the current study [17].

The IGC test results underscore that, even with the use of a buffer layer between the weld and the base metal, excessive heat input during welding can compromise the integrity of the base material. The presence of sensitization, evidenced by the ditch structures observed in the metallographic examinations, highlights localized regions in both the weld and adjacent areas that remain susceptible to intergranular attack [17, 23, 24].

These findings align with the understanding that while buttering can mitigate some risks associated with dissimilar metal welding, it does not fully protect the base metal from the adverse effects of heat input. This underscores the importance of carefully controlling welding parameters to minimize heat input and preserve the mechanical and corrosion-resistant properties of the base material [21].

The results emphasize the need for improved welding practices, specifically through optimizing parameters to reduce heat input. Such measures are essential to prevent sensitization and enhance the overall performance of welded joints made from austenitic stainless steels.

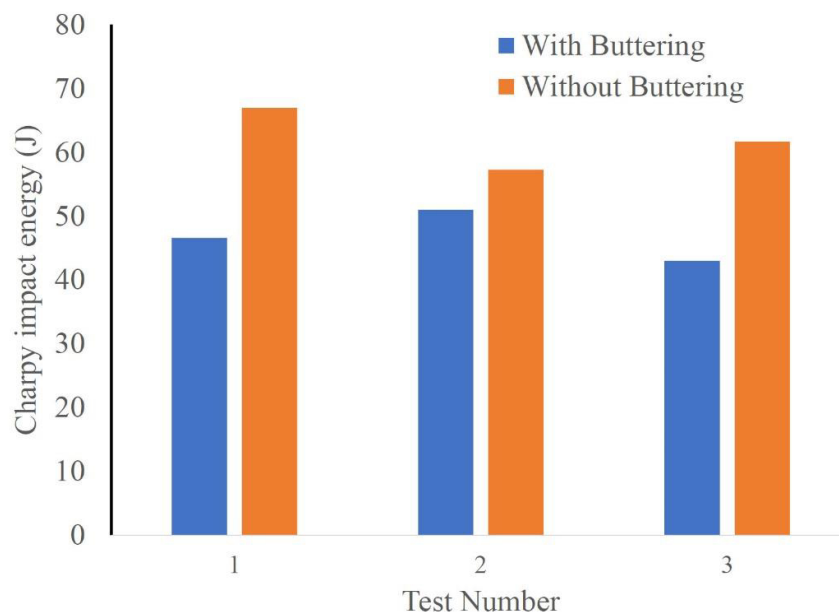


Fig. 11. Charpy impact test results for the buttered and non-buttered samples.

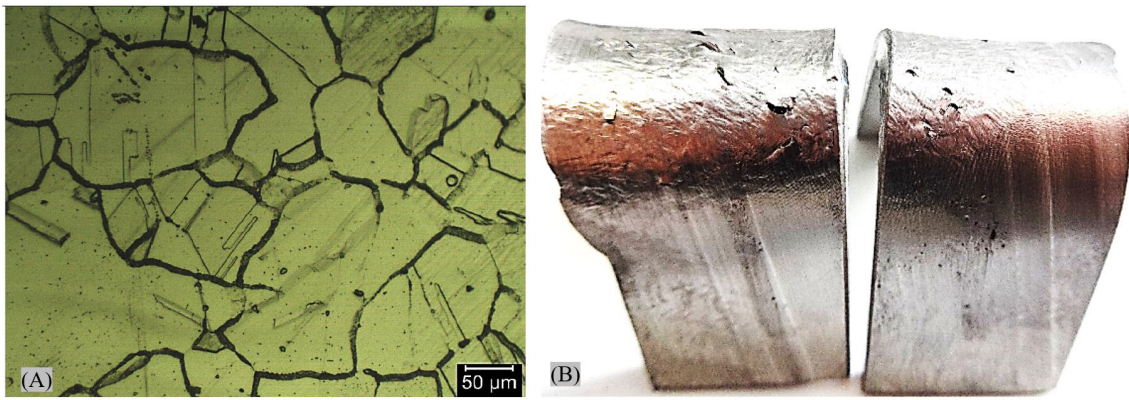


Fig. 12. Test results of IGC test for buttered sample, a) Microstructure after chemical Etching, b) Bending test results as per ASTM A 262 Practice E.

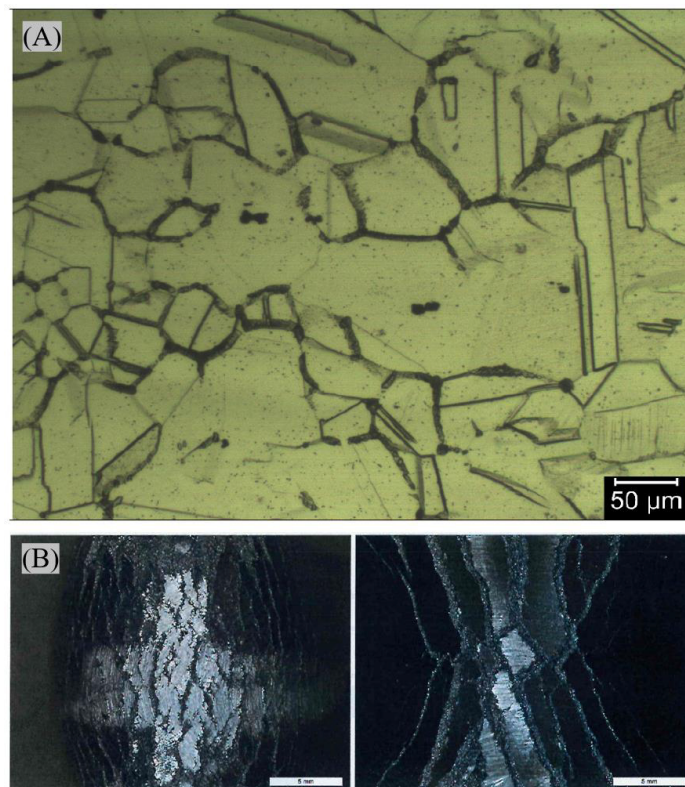


Fig. 13. Test results of IGC test for non-buttered sample, a) Microstructure after chemical Etching, b) Bending test results as per ASTM A 262 Practice E.

4. Conclusions

This study provides a comprehensive analysis of the mechanical properties and corrosion susceptibility of welded Stainless Steel 321H, with a focus on the effects of buttering versus non-buttering techniques. The findings demonstrate that, while buttering offers potential benefits for dissimilar metal welding, it can also present challenges that impact the overall performance of welded joints.

The tensile test results revealed that non-buttered samples generally exhibited superior strength and

ductility compared to the buttered samples, suggesting that the microstructural integrity and uniformity in the non-buttered welds contributed significantly to their better mechanical performance.

Additionally, the impact test results supported these findings, with non-buttered samples showing higher energy absorption values, indicating better toughness under dynamic loading conditions. In contrast, the buttered samples were more prone to cracking under impact loading, highlighting the potential negative effects of introducing additional phases and microstructural

complexities during the buttering process.

The intergranular corrosion tests emphasized the critical importance of controlling welding parameters, as both buttered and non-buttered samples exhibited susceptibility to corrosion. Despite the use of a buttering layer, high heat input during welding led to sensitization in the base metal, compromising its structural integrity.

References

- [1] Gajjar P.K, Khatri B.C, Siddhpura A.M, Siddhpura M.A, Sensitization and desensitization (healing) in austenitic stainless steel: a critical review, *Trans Indian Inst Met.* 2022; 75: 1411-27.
- [2] Kumar S.M, Shanmugam N.S, Studies on the weldability, mechanical properties, and microstructural characterization of activated flux TIG welding of AISI 321 austenitic stainless steel, *Mater Res Express.* 2018; 5(10): 106524.
- [3] American Iron and Steel Institute (AISI), High temperature characteristics of stainless steels. 2004.
- [4] Xu M, Liu B, Dong Z, Wang Z, Influence of microstructure evolution on reheat cracking behavior of T23 steel weld joint, *ISIJ Int.* 2020; 60(6): 1291-300.
- [5] Li Y, Wang J, Wang X, Improvement of stress-relief cracking resistance in coarse-grained heat-affected zones of T23 steel by refining sub-structure through second thermal cycle, *J Mater Res Technol.* 2020; 9(4): 8568-79.
- [6] Bahrami A, Taheri P, A study on the failure of AISI 304 stainless steel tubes in a gas heater unit, *Metals.* 2019; 9(9): 969.
- [7] Chabaud-Reyrtier M, Allais L, Caës C, Pineau A, Mechanisms of stress relief cracking in titanium stabilized austenitic stainless steel, *J Nucl Mater.* 2003; 323(1): 123-37.
- [8] Dayalan I, Crasta P.F, Gupta R, A review on stress relaxation cracking in austenitic stainless steel, In: *Proceedings of the International Conference on Intelligent Manufacturing and Automation*, Springer, Singapore. 2020: 427–34.
- [9] Purnendra B, Chbodenyeva O, Sensitization and its implications for corrosion of austenitic stainless steels in the nuclear industry, *J Nucl Mater.* 2014; 447(1): 14-24.
- [10] Auzoux Q, Allais L, Caës C, Monnet I, Pineau A.F, Effect of pre-strain on creep of three AISI 316 austenitic stainless steels in relation to reheat cracking of weld-affected zones, *J Nucl Mater.* 2010; 400(2): 127-37.
- [11] Bahl S, Dryepondt S, Allard L.F, Suwas S, Shyam A, Retardation of small creep-fatigue crack in Gr. 91 steel through the combined effects of stress relaxation, microstructural evolution, and oxidation, *Metall Mater Trans A.* 2018; 49(12): 6110-21.
- [12] Gupta R.K, Parvathavarthini N, Vinod Kumar A, Dayal R.K, Influence of inclusion and specimen orientations on intergranular corrosion testing of AISI 316LN stainless steel, *Trans Indian Inst Met.* 2017; 64(4): 365-75.
- [13] Zhang S, Jiang Z, Li H, Feng H, Zhang B, Detection of susceptibility to intergranular corrosion of aged super austenitic stainless steel S32654 by a modified electrochemical potentiokinetic reactivation method, *J Alloys Compd.* 2017; 695: 3083-93.
- [14] Liu Y, Zhang X, Liu J, Wang H, Effects of microstructure on mechanical properties of dissimilar metal welded joints, *J Mater Sci Technol.* 2021; 61: 115-30.
- [15] API 942 B-2017, Material, fabrication, and repair considerations for austenitic alloys subject to embrittlement and cracking in high temperature 565°C to 760°C. 2017.
- [16] Sharifi H, Raisi S, Tayebi M, The effect of stress relieving treatment on mechanical properties and microstructure of different welding areas of A517 steel, *Mater Res Express.* 2017.
- [17] Der Westhuizen V, Christian E, Stress relaxation cracking of welded joints in thick sections of a TP347 stabilized grade of stainless steel, *Corrosion.* 2008.
- [18] Blinn M, RA W, Design for fracture toughness, *Mater Sel Des.* 1977; 20: 533-44.
- [19] Prakash K.S, et al. Microstructure, mechanical properties and fracture toughness of SS 321 stainless steel manufactured using wire arc additive manufacturing, *Trans Indian Inst Met.* 2023; 76(2): 537-44.
- [20] Zhu X.K, Joyce J.A, Review of fracture toughness (G, K, J, CTOD, CTOA) testing and standardization, *Eng Fract Mech.* 2012; 85: 1-46.
- [21] Beigi M, Khosravifard A, Rabieezadeh A, Sani R, Effect of microstructural sensitization on mechanical properties of a welded chemically stabilized stainless steel pipe, *J Mater Eng Perform.* 2024.
- [22] Devendranath Ramkumar K, Pavan B, Chandrasekar V, Development of improved microstructural traits and mechanical integrity of stabilized stainless steel joints of AISI 321, *J Manuf Process.* 2018: 582-94.
- [23] Dai P, Li S, Wu L, Wang Y, Feng G, Deng D, A new numerical model to predict welding-induced sensitization in SUS304 austenitic stainless steel joints, *J Mater Res Technol.* 2020; 17: 234-43.
- [24] Ghalambaz M, Abdollahi M, Eslami A, Bahrami A, A case study on failure of AISI 347H stabilized stainless steel pipe in a petrochemical plant, *Case Stud Eng Fail Anal.* 2017; 9: 52-62.